Angiotensin II Pseudopeptides Containing 1,3,5-Trisubstituted Benzene Scaffolds with High AT_2 Receptor Affinity

Jennie Georgsson,[†] Christian Sköld,[†] Bianca Plouffe,[‡] Gunnar Lindeberg,[†] Milad Botros,[§] Mats Larhed,[†] Fred Nyberg,[§] Nicole Gallo-Payet,*[,‡] Adolf Gogoll,[#] Anders Karlén,[†] and Anders Hallberg*[,†]

Department of Medicinal Chemistry, Division of Organic Pharmaceutical Chemistry, Uppsala University, P.O. Box 574, SE-751 23 Uppsala, Sweden, Service of Endocrinology, Faculty of Medicine, University of Sherbrooke, Sherbrooke J1H 5N4, Quebec, Canada, Department of Pharmaceutical Sciences, Division of Biological Research on Drug Dependence, Uppsala University, P.O. Box 591, SE-751 24 Uppsala, Sweden, and Department of Chemistry, Organic Chemistry, Uppsala University, P.O. Box 599, SE-751 24 Uppsala, Sweden

Received March 29, 2005

Two 1,3,5-trisubstituted aromatic scaffolds intended to serve as γ-turn mimetics have been synthesized and incorporated in five pseudopeptide analogues of angiotensin II (Asp-Arg-Val-Tyr-Ile-His-Pro-Phe), replacing Val-Tyr-Ile, Val-Tyr, or Tyr-Ile. All the tested compounds exhibited nanomolar affinity for the AT_2 receptor with the best compound (**3**) having a K_i of 1.85 nM. Four pseudopeptides were AT_2 selective, while one (**5**) also exhibited good affinity for the AT_1 receptor (K_i = 30.3 nM). This pseudopeptide exerted full agonistic activity in an AT_2 receptor induced neurite outgrowth assay but displayed no agonistic effect in an AT_1 receptor functional assay. Molecular modeling, using the program DISCOtech, showed that the high-affinity ligands could interact similarly with the AT_2 receptor as other ligands with high affinity for this receptor. A tentative agonist model is proposed for AT_2 receptor activation by angiotensin II analogues. We conclude that the 1,3,5-trisubstituted benzene rings can be conveniently prepared and are suitable as γ-turn mimics.

Introduction

The octapeptide angiotensin II (Ang II, Asp-Arg-Val-Tyr-Ile-His-Pro-Phe), an important hormone in the renin−angiotensin system, exerts its action by activation of AT_1 and AT_2 receptors. The two receptor types are both G-protein coupled receptors, but they differ considerably by exhibiting a sequence homology of only 32−34% by having distinguished signaling pathways and by having different physiological effects.[1,2] The physiological effects that are most commonly associated with Ang II, e.g., vasoconstriction and aldosteron secretion, are caused by an activation of the AT_1 receptor.[1−3] The AT_2 receptor was cloned in 1993,[4,5] but there are still uncertainties regarding the effects of its activation. Recent studies suggest "anti-AT_1" effects such as vasodilation and hypotension in animal models.[1,6] The AT_2 receptor is also involved in apoptosis, cell differentiation, and tissue repair and in the increase of duodenal mucosal alkalization.[1,2,6−8] In neuronal cells, agonistic activation of the AT_2 receptor induces neurite elongation and outgrowth, modulates neuronal excitability, and promotes cellular migration in adults.[8] The mechanisms involve an activation of the nitric oxide/guanyl cyclase/cGMP pathway[9] and a sustained increase in $p42/p22^{mapk}$ activity.[10]

The natural abundance of AT_2 receptors is very high in the fetus but low in adults, compared to the AT_1 receptor. Notably, the AT_2 receptor is up-regulated in several pathological conditions, e.g., congestive heart failure, renal failure, myocardial infarction, vascular injury, and wound healing.[1,2,6,11]

AT_2 receptor agonists may find a role as therapeutics, e.g., in treatment of hypertension and cardiovascular remodeling.[6,12] The bioactive conformation of Ang II, especially regarding binding to the AT_1 receptor, has been thoroughly studied.[13−18] There are indications that Ang II adopts a γ-turn-like conformation centered at Tyr^4 when binding to and activating the AT_1 receptor based on calculations and rigidifications of Ang II.[19−21] The bioactive conformation of Ang II when binding the AT_2 receptor have so far not been fully investigated. However, photoaffinity labeling experiments suggests an extended β-strand conformation of Ang II when binding to the AT_2 receptor (and also to the AT_1 receptor).[22] Other investigations based on, for instance, computational modeling and binding affinities for the AT_2 receptor of both linear and rigidified Ang II analogues have also been performed that suggest that a turnlike structure may be present in the 3−5 region of Ang II.[23−25] Even less is known regarding the conformations mediating the stimulation of the AT_2 receptor, primarily because of the lack of robust in vitro agonist assays. Cyclizations involving the amino acid residues 3 and 5 in Ang II, e.g., the cyclization delivering the methylenedithioether in **A**[25,26] that induces γ-turn conformations, as well as incorporation of the γ-turn mimicking benzodiazepine scaffolds **B**[23] and **C**[23,24] and the dihydroisoquinolinone scaffold **D**[21] in Ang II, have provided ligands with high affinity for the AT_2 receptor

* To whom correspondence should be addressed. For N.G.-P.: phone, +1-819-564-5243; fax, +1-819-564-5292; e-mail, nicole.gallo-payet@usherbrooke.ca. For A.H.: phone, +46-18-4714284; fax, +46-18-4714474; e-mail, anders.hallberg@orgfarm.uu.se.

[†] Division of Organic Pharmaceutical Chemistry, Uppsala University.

[‡] University of Sherbrooke.

[§] Division of Biological Research on Drug Dependence, Uppsala University.

[#] Department of Chemistry, Organic Chemistry, Uppsala University.

10.1021/jm050280z CCC: $30.25
Published on Web 09/23/2005

Chart 1

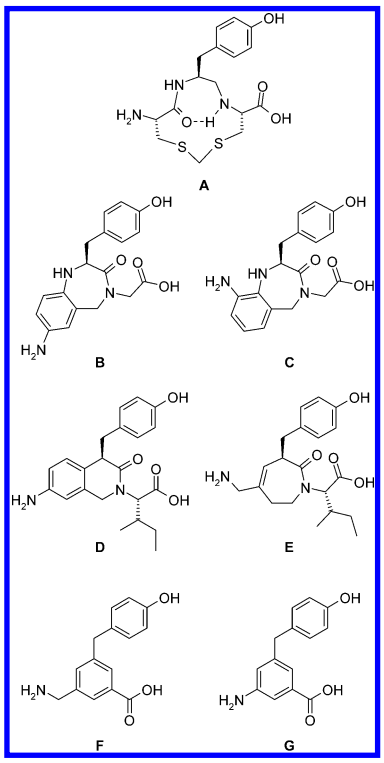

(Chart 1). Some of these ligands were recently shown to exert agonistic activity at the AT_2 receptor.[24]

Whereas the pseudopeptides incorporating **B**, **C**, or **D** in the 3−5 region of Ang II did not bind to the AT_1 receptor, the analogues containing **A** and the azepine γ-turn mimic **E** showed affinity for the AT_1 receptor.[21,25,26] Furthermore, a pseudopeptide with the 1,3,5-trisubstituted benzene **F**, representing a more compact γ-turn scaffold in the 3−5 region of Ang II, was found to lack all AT_1 receptor affinity.[27] It seems that the AT_1 receptor responds to small variations of the turn geometry in the 3−5 region of Ang II while the AT_2 receptor is less sensitive. Accordingly, we speculated that pseudopeptides encompassing the synthetically easily accessible γ-turn scaffolds **F** and the even more compact **G** might serve as good AT_2 receptor ligands.

Herein, we report the synthesis of the two γ-turn mimetic scaffolds **F** and **G**, each with an aromatic ring as a common core structure, and the synthesis of five peptide analogues of Ang II (Chart 2) containing these two scaffolds. We disclose that pseudopeptides comprising the aromatic scaffold **G** can exhibit high AT_1 and AT_2 receptor affinity while those containing **F** demonstrate high AT_2 receptor selectivity. One of the Ang II analogues was found to act as a full AT_2 receptor agonist.

Results

Chemistry. Compound **12** was previously synthesized by us, although with the phenolic hydroxy group Fmoc-protected and by a procedure delivering a considerably lower total yield.[27] The synthetic route to intermediates **8a**,**b** is outlined in Scheme 1, and the preparation of templates **12** and **15** is in Schemes 2 and 3, respectively.

Compounds **7a**,**b** were prepared by Friedel−Crafts acylation of anisole using the acid chlorides of the commercially available benzoic acid derivatives **6a**,**b**. In the acylation step, the ortho/para ratios were found to be highly substrate-dependent, providing high para selectivity from **6a** but not from **6b**.[28] The benzophenone **7a** was isolated as the pure para derivative in 73% yield by simple crystallization. The same synthetic transfor-

Chart 2

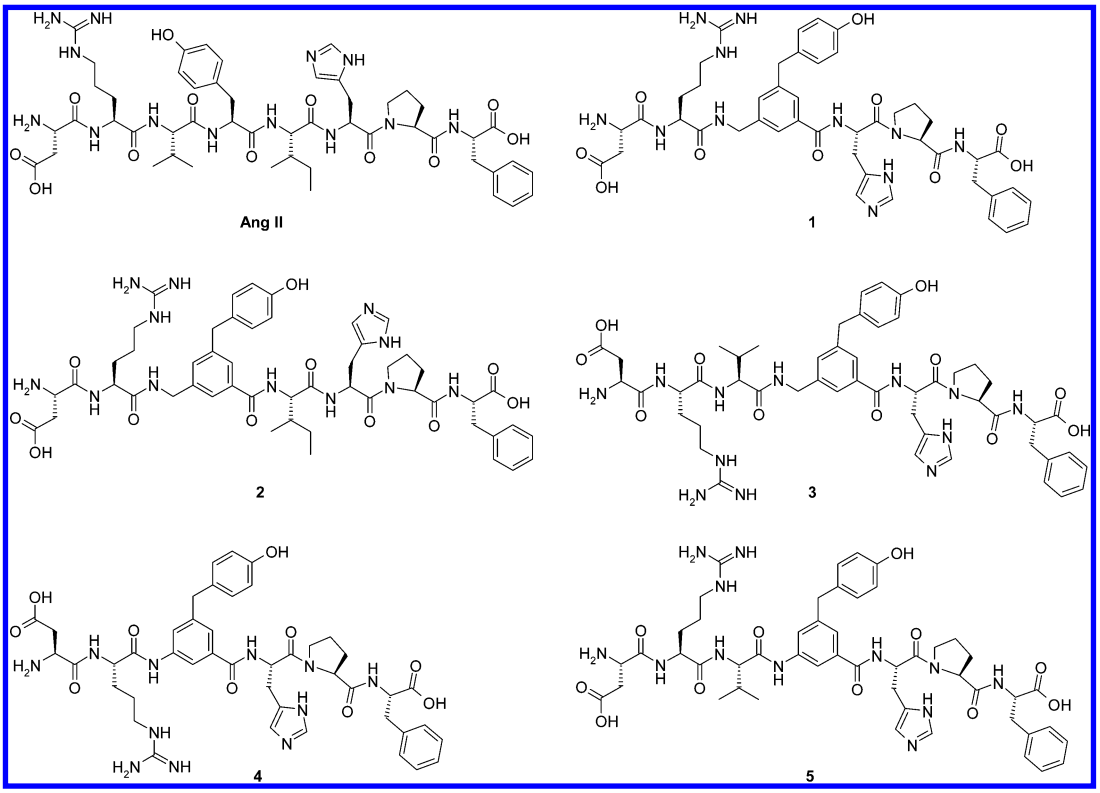

Scheme 1[a]

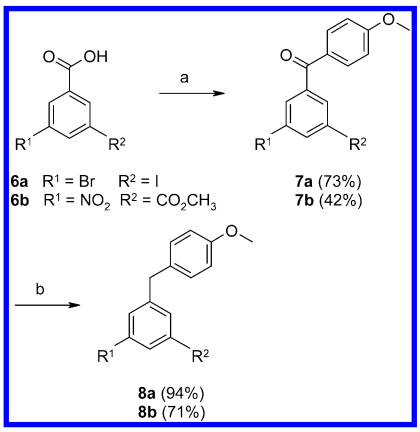

[a] Reagents: (a) (i) $SOCl_2$, reflux; (ii) anisole, $AlCl_3$, DCM; (b) $(CH_3CH_2)_3SiH$, F_3CSO_3H, TFA, DCM.

Scheme 2[a]

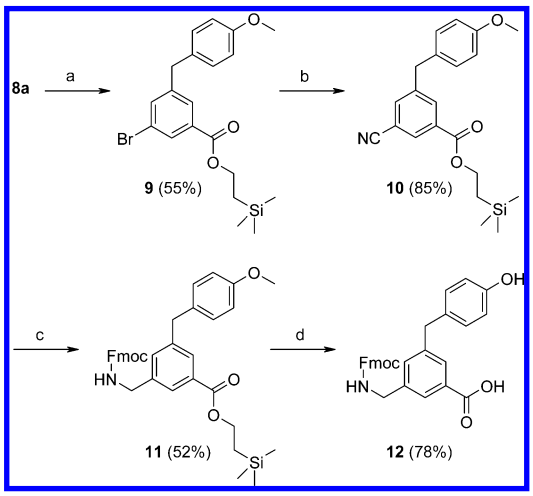

[a] Reagents: (a) $Mo(CO)_6$, Pd/C, DMAP, DIEA, $HOCH_2CH_2Si(CH_3)_3$,dioxane, microwave heating, 130 °C, 15 min; (b) $Zn(CN)_2$, $Pd_2(dba)_3$, P(*o*-tolyl)$_3$, DMF, microwave heating, 180 °C, 10 min; (c) (i) H_2, Pd/C, EtOH; (ii) Fmoc-Cl, aqueous Na_2CO_3, dioxane; (d) $BF_3{\cdot}S(CH_3)_2$, DCM.

Scheme 3[a]

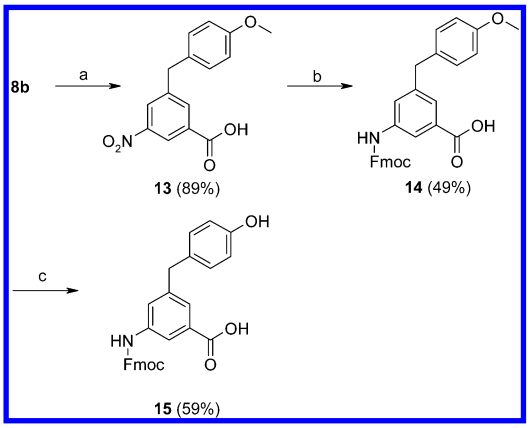

[a] Reagents: (a) LiOH, THF/MeOH/H_2O; (b) (i) H_2, Pd/C, EtOH; (ii) Fmoc-Cl, aqueous Na_2CO_3, dioxane; (c) $BF_3{\cdot}S(CH_3)_2$, DCM.

mation to obtain **7b** required additional optimization, and a preactivation of the acid chloride with the $AlCl_3$ was found to be beneficial. Despite this improvement, only approximately 65% conversion was achieved after 5 days at ambient temperature. Thus, the ortho and para isomers were separated by column chromatography, and **7b** was isolated in 42% yield. The subsequent high-yielding reduction of ketones **7a**,**b** to form **8a**,**b** was conducted under acidic conditions in DCM, employing triethylsilane as the hydride source.[29−31] It was essential to conduct the carbonyl reduction at this stage, since it was found to be remarkably difficult to perform subsequent palladium(0)-catalyzed coupling reactions with an intact acyl substituent.

The ester functionality in **9** was introduced by a microwave-assisted palladium-catalyzed alkoxy carbonylation (Scheme 2).[32] In this protocol, $Mo(CO)_6$ was utilized as a solid carbon monoxide source and palladium on charcoal was used as a catalyst without extra addition of phosphine ligands. With substrate **8a**, the reactivity of the iodide was considerably higher than for the bromide and thus allowed chemoselective introduction of the ester-protected carboxylic acid function despite the high temperature (130 °C). The major side product, as deduced from GC−MS, was the dehalogenated starting material. To obtain compound **10**, a palladium-catalyzed cyanation was performed using a microwave-accelerated procedure.[33,34] $Pd_2(dba)_3$ and tri-*o*-tolylphosphine provided the catalytic system in situ and $Zn(CN)_2$ served as the cyanide source. To attain reproducible results, it was crucial to keep the amount of $Zn(CN)_2$ low to avoid poisoning of the catalyst.[35] A standard hydrogenation of nitrile **10** under an atmospheric pressure of hydrogen gas employing palladium on charcoal in absolute ethanol smoothly generated the benzylamine, which was subsequently reacted with Fmoc chloride in a solution of aqueous Na_2CO_3 and dioxane to produce **11**.[36] Simultaneous cleavage of the TMSE ester and the methoxy group was accomplished with a boron trifluoride dimethyl sulfide complex in DCM to afford the Fmoc-protected γ-turn scaffold **12**.[37]

Compound **13** was synthesized by hydrolysis of compound **8b** with LiOH in THF/H_2O/MeOH. The conditions described above for the preparation of compound **11** were thereafter used for reduction of the nitro group of **13** and the subsequent Fmoc protection to produce compound **14**. The final deprotection of the hydroxyl function to produce the Fmoc-protected γ-turn template **15** was conducted as described above for the preparation of **12**. The scaffolds **F** and **G** were introduced in the pseudopeptides as their Fmoc-protected equivalents **12** and **15**. The pseudopeptides **1**−**5** were synthesized by standard Fmoc strategy solid-phase peptide synthesis (SPPS) using standard SPPS with PyBOP as the coupling reagent. The introduced γ-turn mimetic scaffolds **F** and **G** replaced Val-Tyr-Ile in compounds **1** and **4**, Tyr-Ile in **3** and **5**, and Val-Tyr in **2**.

NMR signal assignment was obtained following routine methodology, revealing connectivity within amino acid residues by primitive exclusive correlation spectroscopy (PE COSY)[38] and total correlation spectroscopy (TOCSY)[39] experiments and sequential assignments from rotating-frame Overhauser enhancement spectroscopy (ROESY)[40] experiments. These experiments were combined with solvent suppression by the wet technique.[41] Chemical shift data are available in Supporting Information.

At room temperature, the spectra of the peptidomimetics **3** and **4** indicate the presence of two conformers due to cis−trans isomerism of the proline peptide bond.

Table 1. Binding Affinities for the AT_1 and AT_2 Receptors

compd	AT_1 (rat liver membranes) $K_i \pm$ SEM (nM)	AT_2 (pig uterus myometrium) $K_i \pm$ SEM (nM)
Ang II	0.95 ± 0.08	0.2
[Sar[1]]Ang II	0.16 ± 0.03	0.18 ± 0.01
[4-NH_2-Phe[6]]Ang II	>10000	0.7
1	>10000	10.1 ± 0.6
2	>10000	463.7 ± 10.9
3	>10000	1.85 ± 0.1
4	>10000	41.3 ± 0.8
5	30.3 ± 1.5	9.8 ± 0.3

As expected, the number of signals is reduced when the temperature is increased (to 60 °C) because of the faster exchange between isomers at elevated temperature.

Binding Assay. Compounds **1**−**5** were evaluated in radioligand binding assays relying on displacement of [^{125}I]Ang II from AT_1 receptors in rat liver membranes[42] and from AT_2 receptors in pig uterus membranes[43] (Table 1). Ang II, [4-NH_2-Phe[6]]Ang II, and [Sar[1]]Ang II were used as reference substances. The results are summarized in Table 1. All compounds showed affinity for the AT_2 receptor, and one compound also showed affinity for the AT_1 receptor. The pseudopeptide **1** with the scaffold **F** replacing Val-Tyr-Ile in Ang II displayed a K_i of 10.1 nM for the AT_2 receptor. When **F** replaced the two amino acids Val-Tyr (**2**), a 40-fold drop in affinity was observed compared to **1**. The highest affinity for the AT_2 receptor was encountered with compound **3** (K_i = 1.85 nM) where **F** replaces Tyr-Ile. Scaffold **G** was introduced in compounds **4** and **5** as a substitute for Val-Tyr-Ile and Tyr-Ile, respectively. Compound **4** had moderate affinity for the AT_2 receptor (K_i = 41.3 nM). Notably, compound **5** exhibited affinity for both the AT_1 and the AT_2 receptors. This substance was further evaluated in functional AT_1 and AT_2 assays to elucidate whether it serves as an agonist to these receptors.

In Vitro Morphological Effects Induced by Compound 5 in NG 108-15 Cells. To study the effect of pseudopeptide **5** on morphological differentiation, i.e., neurite outgrowth, NG108-15 cells were used. In their undifferentiated state, neuroblastoma−glioma hybrid NG108-15 cells have a rounded shape and divide actively. We have previously shown that these cells exclusively express the AT_2 receptor[44,45] and exhibit long neurites after a 3-day treatment with Ang II or the selective peptide agonist CGP 421112.[45] After a 3-day treatment, pseudopeptide **5** induced neurite outgrowth and most cells extended one or two neurite processes, exhibiting a growth cone at the tip, while the cell body retained a rounded appearance. Compared to Ang II at the same concentration, pseudopeptide **5** induced the same morphological changes as previously shown.[45]

Quantification indicated an increase in the number of cells with neurites longer than the cell body from 3.8% ± 0.2% in control cells to 14.3% ± 0.2% in cells treated with compound **5** (Figure 1). Incubation of **5** with the AT_2 receptor antagonist PD 123,319 (1.0 μM) halted the neurite elongation. We have previously shown that PD 123,319 did not alter the morphology of the untreated cells.[10,45]

Rabbit Thoracic Aorta String, AT_1 Functional Assay. Compound **5** was tested for agonist activity at seven concentrations ranging from 3.0 nM to 3.0 μM at the AT_1 receptor in the rabbit thoracic aorta with the agonist angiotensin II as reference according to literature procedure.[46] Angiotensin II induced a concentration-dependent contraction of the rabbit thoracic aorta, which was inhibited by the AT_1 receptor antagonist saralasin. Unlike Ang II, compound **5** did not produce any contraction of this tissue at a concentration as high as 3.0 μM.

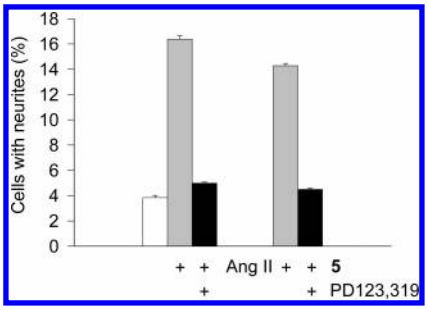

Figure 1. Effect of the AT_2 receptor antagonist PD 123,319 on pseudopeptide **5** induced neurite outgrowth in NG108-15 cells. Cells with at least one neurite longer than the cell body were counted as positive for neurite outgrowth. The number of cells with neurites represents the percentage of the total number of cells in the micrographs (from 67 to 186 cells according to the experiment): control, with Ang II (0.1 μM) stimulation, Ang II (0.1 μM) in the presence of PD 123,319 (1.0 μM), **5** (0.1 μM), and **5** (0.1 μM) in the presence of PD 123,319 (1.0 μM).

Comparison of Scaffolds F and G to Peptide γ-Turns. Conformational analysis of compounds **F** and **G** modified with an N-terminal acetyl cap, C-terminal *N*-methylamide cap, and an alanine side chain instead of the tyrosine side chain resulted in eight and four conformations, respectively, within 5 kcal/mol of the lowest energy minimum. The identified conformations were evaluated by least-squares alignment of the scaffolds to γ-turns from an in-house database of 2101 extracted inverse γ-turns from crystallized protein structures from the PDB.[47] Conformations from both scaffolds were superimposed with a low root-mean-square (rms) value onto many of the inverse γ-turns in the database; 586 and 347 inverse γ-turns could be superimposed onto a conformation of **F** and **G**, respectively, with an rms value less than 0.5 Å. One example is shown as a stereo image in Figure 2 (rms = 0.11 and 0.29 Å for **F** and **G**, respectively, superimposed onto a protein γ-turn from PDB 1EUV, chain A, Pro[596]-Leu[597]-Asp[598], Leu[597], as amino acid i + 1).

DISCOtech Analysis. To study if the compounds with high affinity for the AT_2 receptor could adopt similar binding modes, the pharmacophore modeling program DISCOtech[48] was used. Compounds **1m**, **3m**, and **5m** (Chart 3) served as models for **1**, **3**, and **5**. The model compounds **16m**, **17m**, and **18m** were also included in the analysis (see ref 24 for the structures of the parent compounds, which have high affinity for AT_2 receptors). DISCOtech identified 316 different models with superimposed conformations where the selected structural elements were positioned in the same regions in space. Some of the models had a low overall structural overlap and were therefore not considered further. Many of the models were also redundant because they had very similar alignments. DISCOtech was set to produce models with all or all but one compound included. It seems that it was difficult to make models

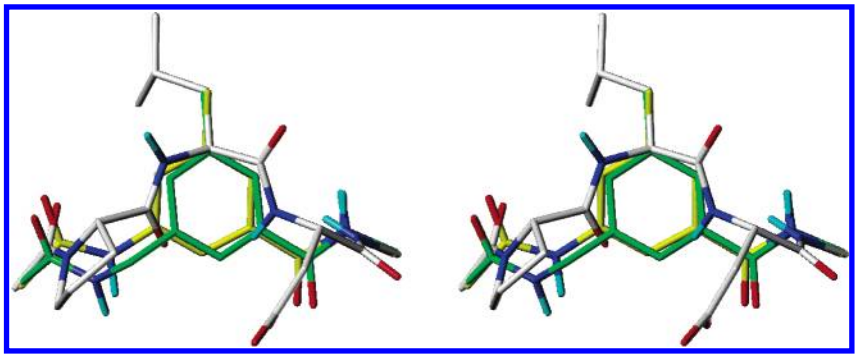

Figure 2. Stereo image of models of scaffolds **F** (green carbons) and **G** (yellow carbons) superimposed onto an inverse γ-turn found in a crystallized protein.

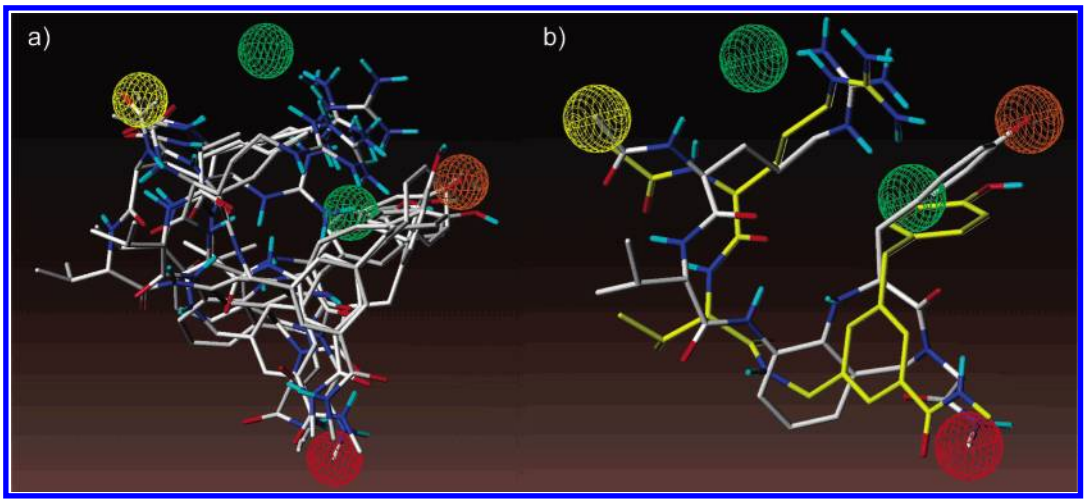

Figure 3. (a) DISCOtech model including all compounds. (b) Same model but with only **3m** (yellow carbons) and **17m** (white carbons) displayed. Spheres indicate the DISCOtech features: yellow, N-terminal; red, C-terminal; orange, tyrosine phenolic oxygen; green, proposed receptor interaction point for the arginine guanidino group. The proposed interaction point located in the area occupied by the tyrosine side chain should be ignored.

Chart 3

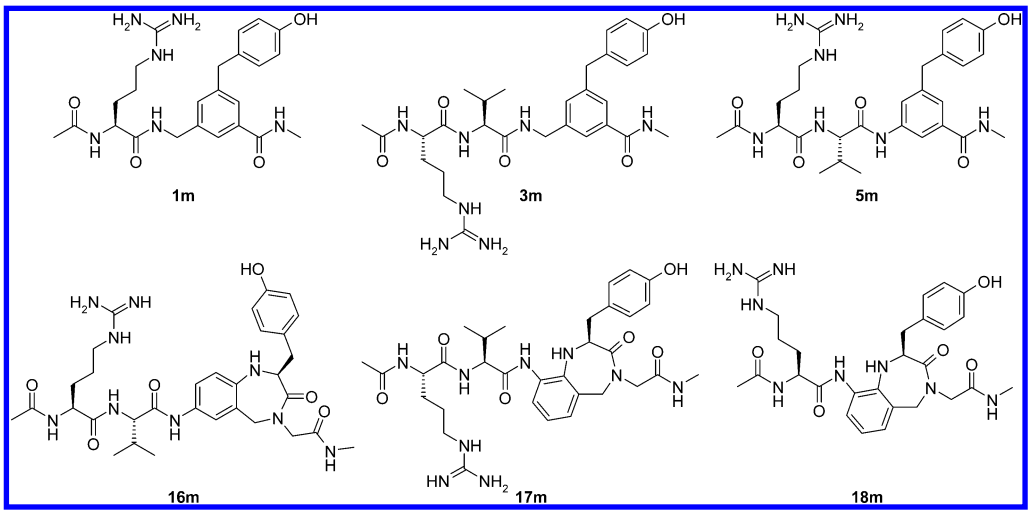

that included **16m**, since it was omitted from most models. One of the few models with all compounds reasonably aligned is shown in Figure 3 where each of the four investigated structural elements are confined within 2.0 Å from each other. Since DISCOtech does not consider structural information, the proposed interaction point of the guanidino group found in the area occupied by the tyrosine side chain should therefore be ignored. The other proposed interaction point is more realistic. A DISCOtech analysis was also made using only the AT_2 receptor agonist model compounds **5m**, **16m**, **17m**, and **18m**. DISCOtech found 145 models. Interestingly only one of these included all four agonists. This model was very similar to the one presented in Figure 3. In the remaining models only three of the four compounds were included.

Discussion

The first selective non-peptide AT_1 receptor agonist was discovered in 1994.[49] Recently, we reported the first

nonpeptidic selective AT_2 receptor agonist.[50] Both these agonists, which are structurally similar to the "sartans", originate from a nonselective AT_1/AT_2 agonist.[51] The synthetic optimization to afford the druglike AT_2 receptor ligand was performed by classical medicinal chemistry methodology. In parallel, we are addressing the challenging task of systematically transforming Ang II to a more druglike molecule by a process where the determination and examination of essential recognition elements in the bioactive conformation are key components. An important tool is amino acid scans that can early reveal valuable information on essential elements. The Arg^2 residue seems to contribute to the binding affinity to the AT_2 receptor, but considering this receptor, no particular amino acid is crucial for binding.[52,53] Furthermore, replacing parts in the backbone of the natural peptide by well-defined secondary structure motifs constitutes a basic strategy in such an iterative process.

There is support that Ang II adopts a γ-turn-like conformation in the 3−5 region when binding to the AT_1 receptor. In the binding of Ang II to the AT_2 receptor, an extended β-strand conformation has been suggested in addition to turnlike motifs. These two hypotheses do not necessarily have to be in conflict with each other, since a reasonable extended conformation might be adopted even with a turn-mimicking scaffold present in the central part of the pseudopeptide. We have therefore probed this region in Ang II and introduced the slightly geometrically different monocyclic and bicyclic γ-turn mimetic scaffolds shown in Chart 1 and measured the affinity of the pseudopeptides. Only one of the synthesized analogues (built around scaffold **E**) showed affinity ($K_i = 2.8$ nM) and agonist activity at the AT_1 receptor. In contrast, several pseudopeptides prepared displayed high affinity for the AT_2 receptor.

We previously showed that the 1,3,5-trisubstituted benzene γ-turn scaffold, when introduced in Ang II to give **1** and **2**, delivered pseudopeptides inactive at the AT_1 receptor.[27] We have now resynthesized these compounds using a modified and more efficient route to the core structure. In the design of these compounds the side chain of Val^3 was deleted. It is assumed that Val^3 has only a conformationally stabilizing role in Ang II and thus can be removed in the γ-turn mimetics. Furthermore, since it is unclear what to introduce at the C-terminal end of this scaffold, we coupled both His-Pro-Phe and Ile-His-Pro-Phe to give **1** and **2**.[27] Compounds **1** and **2** were reevaluated in the binding assay, and the lack of affinity for the AT_1 receptor was confirmed. In contrast, in the AT_2 receptor-binding assay these compounds exhibited K_i values of 10.1 and 463.7 nM, respectively. Apparently, the introduction of the isoleucine residue between scaffold **F** and the C-terminal provided a pseudopeptide (**2**) with 2300 times weaker affinity than Ang II for the AT_2 receptor. In contrast, compound **1** lacking the isoleucine residue is only 10 times less potent than Ang II. Thus, the 1,3,5-trisubstituted scaffold seems to be a better mimic of Val-Tyr-Ile than Val-Tyr. With knowledge about the preferred C-terminal of these peptides for binding to the AT_2 receptor, we set out to optimize the N-terminal part. Our previous SAR studies of pseudopeptides interacting with the AT_2 receptor have shown that a valine residue inserted between the arginine and the γ-turn mimetic can improve receptor interaction.[23,24] Compound **3** was therefore synthesized and was found to provide a 5 times higher affinity for the AT_2 receptor compared to **1**.

In the benzodiazepine γ-turn mimetics **B** and **C**, the nitrogen is linked directly to the benzene ring, while in the trisubstituted benzene γ-turn mimetic **F**, a methylene group separates the nitrogen from the aromatic ring. To study how **G**, where the 1,3,5-trisubstituted benzene scaffold with the nitrogen attached directly to the benzene ring, compares to γ-turns in proteins, we searched an in-house database of γ-turns derived from the PDB and superimposed these onto low-energy conformations of a model structure of the scaffold. A model structure of **F** was also included in the comparison. Even though the aromatic ring is smaller compared to the peptide γ-turn, the C_α of the $i - 1$ residue, the C_α of the $i + 3$ residue, and the side chain of the $i + 1$ residue align reasonably well. This indicates that both **F** and **G** may replace the inverse γ-turn structure. Since the core structure **G** is also accessible via a synthetic route similar to the one used for **F**, we synthesized pseudopeptides **4** and **5**. In the AT_2 receptor-binding assay, these pseudopeptides displayed only a somewhat lower affinity than **3**, which further supports the finding that the AT_2 receptor is quite tolerant toward changes in the 3−5 region of Ang II.

In pseudopeptides **1** and **4** the core structures replace the amino acid residues Val-Tyr-Ile. These two compounds bind to the AT_2 receptor with a somewhat lower affinity compared to Ang II. However, when Val^3 is also introduced (compounds **3** and **5**), the affinity is improved by 4−5 times. The extra valine residue may have introduced extra flexibility and enabled more favorable binding interactions of the pseudopeptides with the AT_2 receptor. The same impact of an incorporation of Val^3 was also observed for the corresponding benzodiazepine-based γ-turn mimetics introduced in the same region in Ang II.[24]

Several of the models identified by DISCOtech had all of the key groups in the same region and also had a reasonable overall alignment of the scaffolds (Figure 3a). In Figure 3b only **3m** and **17m** are shown for clarity. This model is very similar to the one previously published, which was based on only **16m**, **17m**, and **18m**, which are all based on a benzodiazepine scaffold. It thus seems possible to find a common alignment of key groups in the pseudopeptides incorporating a 1,3,5-trisubstituted benzene scaffold and a 7- or 9-substituted benzodiazepine. DISCOtech models based on only the four AT_2 receptor agonists (**5m** **16m**, **17m**, and **18m**) were also produced. Interestingly only one model could be identified that included all four agonists. This model was geometrically very similar to the one based on the six compounds with high affinity (Figure 3). However, more AT_2 receptor agonists are needed to validate and explore this model further.

We found it surprising that compound **5** (lacking Ile^5) showed affinity for the AT_1 receptor (AT_1 $K_i = 30.3$ nM). In fact, out of the many γ-turn-like mimetics synthesized and introduced in Ang II, only one has resulted in affinity for the AT_1 receptor. It is not straightforward to rationalize the present findings because, for example,

the only difference between **5** and **3** (devoid of AT_1 receptor affinity) is the methylene group between the nitrogen and the aromatic ring. Thus, subtle differences in the ligands seem to be of key importance for obtaining high AT_1 receptor affinity.

Conclusion

Herein, we described straightforward synthetic routes to the two small aromatic scaffolds **F** and **G**, both of which proved to be useful peptidomimetic core structures. Molecular modeling supports the view that 1,3,5-trisubstituted aromatic scaffolds may serve as relevant γ-turn mimetics. The scaffolds **F** and **G** were used as substitutes for the tripeptide Val-Tyr-Ile or for the dipeptides Tyr-Ile and Val-Tyr in the proposed turn in order to find the optimal position of the scaffolds for this class of compounds. All five pseudopeptides exhibit nanomolar affinities for the AT_2 receptor, confirming that considerable differences in the central part of Ang II are tolerated at this receptor. In contrast, minor changes have a great impact on the AT_1 receptor affinity and thereby the selectivity. Functional assays established that the nonselective AT_1/AT_2 receptor ligand **5** is a full agonist at the AT_2 receptor but lacks agonistic activity at the AT_1 receptor. Molecular modeling confirms that the model based on only the confirmed agonists is very similar to the one with all six high-affinity ligands included. Thus, a tentative model is proposed for activation of the AT_2 receptor by angiotensin II analogues.

Experimental Section

General. ^{1}H NMR and ^{13}C NMR were obtained on a JEOL JNM-400 spectrometer (^{1}H at 400 MHz, ^{13}C at 100.6 MHz) or on a Varian Mercury plus spectrometer (^{1}H at 400 MHz, ^{13}C at 100.6 MHz). Spectra were recorded at ambient temperature unless otherwise stated. Chemical shifts are reported as δ values (ppm) referenced to δ 7.26 ppm for $CHCl_3$, δ 77.0 ppm for $CDCl_3$, δ 2.05 ppm and δ 29.84 ppm for acetone-d_6, and δ 1.94 and 1.32 ppm for MeCN-d_3. NMR spectra for the pseudopeptides were recorded on a Varian UNITY INOVA (^{1}H at 499.9 MHz) spectrometer. Signal assignment was made using PE COSY,[38] TOCSY,[39] and ROESY[40] experiments, using solvent suppression with the wet[41] technique. A mixing time of 0.4 s was used for the ROESY experiments. IR spectra were generated on a Fourier transform IR spectrometer. GC−MS was performed with an electron impact (70 eV) mass-selective detector and a HP-1 capillary column using a 70−305 °C temperature gradient. Analytical RP-LC−MS was performed on a Gilson HPLC system with a Finnigan AQA quadropole mass spectrometer using a Chromolith Performance RP-18 100 mm × 4.6 mm column (Merck) at a flow rate of 4 mL/min. Preparative RP-HPLC was performed with a Zorbax SB-C8, 5 μm, 150 mm × 21.2 mm column (Agilent Technologies) at a flow rate of 12 mL/min. The pseudopeptide purities were determined on a Thermo Hypersil HyPurity C4, 5 μm, 4.6 mm × 50 mm column and a ACE 5 C18, 4.6 mm × 50 mm column. MikroKemi AB, Uppsala, Sweden, or Analytische Laboratorien, Industriepark Kaiserau, Lindlar, Germany, performed elemental analyses. Molecular masses (HRMS) were determined on a Micromass Q-Tof2 mass spectrometer equipped with an electrospray ion source. The microwave heating was conducted in a Smith synthesizer system at a frequency of 2450 MHz under noninert conditions. Column chromatography was performed using commercially available silica gel 60 (particle size: 0.040−0.063 nm, Merck). Thin-layer chromatography performed with aluminum sheets coated with silica gel 60 F_{254} (0.2 mm, E. Merck), and the analytes were visualized with UV light. Dichloromethane used in the reactions was distilled over calcium hydride. Other chemicals were used without further purification. The AT_1 functional assay was performed at Cerep, France.

3-Bromo-5-iodo-4′-methoxybenzophenone (7a). The commercially available 3-bromo-5-iodobenzoic acid (9.9 g, 30.4 mmol) was refluxed in 60 mL of thionyl chloride for 1 h. The thionyl chloride was evaporated under reduced pressure. The crude product was dissolved in 160 mL of dry DCM, and anisole (9.9 mL, 91.2 mmol) was added. $AlCl_3$ (8.0 g, 60.8 mmol) was added in portions over 30 min. The reaction mixture was stirred at room temperature overnight and was then poured into a mixture of 100 mL of ice and 150 mL of 1 M HCl and extracted with DCM. The organic phase was washed with water and brine, dried over $MgSO_4$, and evaporated. Crystallization from ethanol afforded the para product **7a** as off-white crystals (9.23 g, 73%). Anal. ($C_{14}H_{10}BrIO_2$) C, H.

1-Bromo-3-iodo-5-(4-methoxybenzyl)benzene (8a). A solution of **7a** (9.0 g, 21.6 mmol) in 150 mL of dry DCM was cooled to 0 °C, and TFA (16.6 mL, 216 mmol) and triflic acid (50 μL, 0.52 mmol) were added. Triethylsilane (10.3 mL, 64.7 mmol) was added dropwise with an addition funnel to the solution. The ice bath was removed, and the reaction mixture was refluxed for 6 h, then washed with 1 M NaOH and brine, dried over $MgSO_4$, and evaporated. Compound **8a** was isolated as an off-white solid (8.22 g, 94%). Anal. ($C_{14}H_{12}BrIO$) C, H.

(2-Trimethylsilanylethyl)-3-bromo-5-(4-methoxybenzyl)-benzoate (9). Each of 13 microwave 2−5 mL vials was charged with a stirring bar, palladium on charcoal (10%, 80 mg, 0.08 mmol), and $Mo(CO)_6$ (411 mg, 1.55 mmol). A solution of **8a** (8.16 g, 20.2 mmol) and DMAP (2.5 g, 20.5 mmol) in 44 mL of dioxane was divided into 13 aliquots and added to the microwave vials. DIEA (0.77 mL, 4.4 mmol) and 2-(trimethylsilyl)ethanol (1.0 mL, 7.0 mmol) were added to each vial, which was sealed under air. The samples were agitated and heated sequentially by microwave irradiation to 130 °C for 15 min. After cooling, the reaction mixtures were filtered, pooled, and concentrated in vacuo. The crude product was diluted with EtOAc, washed with 5% citric acid, water, and brine, dried over $MgSO_4$, and evaporated. The residue was purified by column chromatography on silica with 40% isohexane in DCM as the mobile phase to give **9** as a clear oil (4.73 g, 55%). Anal. ($C_{20}H_{25}BrO_3Si$) C, H, N.

(2-Trimethylsilanylethyl)-3-cyano-5-(4-methoxybenzyl)-benzoate (10). Each of 10 microwave 2−5 mL vials was charged with a stirring bar and $Zn(CN)_2$ (36 mg, 0.31 mmol). A 25 mL stock solution of **9** (2.12 g, 5.0 mmol) in DMF was prepared, and aliquots of 2.5 mL were added to each of 10 microwave vials precharged with $Pd_2(dba)_3$ (10.5 mg, 12 nmol) and P(*o*-tolyl)$_3$ (15 mg, 48 nmol) in DMF (2 mL). After 15 min, the reaction mixture was added to a microwave vial, sealed, and immediately heated to 180 °C for 10 min. After cooling, all 10 reaction mixtures were combined and poured into 2 M NH_4OH (250 mL). The product was subsequently extracted into EtOAc. The combined organic phases were washed with water and brine, dried with Na_2SO_4, and evaporated under reduced pressure. The crude product was purified on a silica column with DCM/isohexane (1:1) as the mobile phase to give compound **10** (1.57 g, 85%). Anal. ($C_{21}H_{25}NO_3Si$) C, H, N.

(2-Trimethylsilanylethyl)-3-[(9*H*-fluoren-9-ylmethoxy-carbonylamino)methyl]-5-(4-methoxybenzyl)benzoate (11). A round-bottom flask was charged with a stirring bar and palladium on charcoal (10%, 404mg, 0.38 mmol). A solution of **10** (1.4 g, 3.8 mmol) in absolute ethanol (70 mL) was added, and the flask was sealed with a septum and purged, first with nitrogen and then with hydrogen gas. The reaction mixture was stirred under hydrogen at atmospheric pressure for 80 min and was then filtered and evaporated. The crude product was analyzed by GC−MS and found to be adequate for further reaction. The generated amine (3.8 mmol) was dissolved in dioxane (50 mL) and cooled in an ice bath. A 10% aqueous solution of Na_2CO_3 (100 mL) was added slowly. Fmoc chloride (1.47 g, 5.7 mmol), dissolved in dioxane (50 mL), was added dropwise to the reaction mixture, which was

allowed to reach ambient temperature under stirring for 4 h. Water (100 mL) was added, and the mixture was extracted with ethyl acetate. The organic phase was washed with water and brine, dried over $MgSO_4$, and evaporated. The product was purified on a silica column using 5% ethyl acetate in toluene. Compound **11** was isolated as a clear oil (1.17 g, 52%). Anal. ($C_{36}H_{39}NO_5Si$) H, N. C: calcd, 72.82; found, 73.6.

3-[(9*H*-Fluoren-9-ylmethoxycarbonylamino)methyl]-5-(4-hydroxybenzyl)benzoic Acid (12). Compound **11** (591 mg, 1.0 mmol) was dissolved in dry DCM (15 mL). The reaction vessel was fitted with a septum and cooled in an ice bath. $BF_3 \cdot S(CH_3)_2$ (1.1 mL, 10.0 mmol) was added slowly to the solution. The reaction mixture was allowed to reach ambient temperature and was left stirring overnight. It was then poured into water and extracted with ethyl acetate. The organic phase was extracted with 1 M K_2CO_3. The aqueous phase was acidified with 6 M HCl and extracted with ethyl acetate. The organic phase was then dried over $MgSO_4$ and evaporated to give **12** (376 mg, 78.4 mmol) as a clear oil in 78% yield. Anal. ($C_{30}H_{25}NO_5$) C, H, N.

3-(4-Methoxybenzoyl)-5-nitromethylbenzoate (7b). 5-Nitroisophthalic acid monomethyl ester (3.0g, 13.3 mmol) was refluxed in 20 mL of thionyl chloride for 1 h. The thionyl chloride was evaporated under reduced pressure and kept under vacuum overnight. The crude product was dissolved in 25 mL of dry DCM. $AlCl_3$ (5.32 g, 39.9 mmol) was suspended in 15 mL of DCM and cooled to 0 °C. The solution of the acid chloride was added slowly to the suspension, and the reaction mixture was stirred at 0 °C for 30 min. Anisole (1.9 mL, 17.5 mmol) was added dropwise, and the temperature was raised to room temperature. After 4 h another portion of anisole (2.45 mL, 22.5 mmol) was added, and the mixture was stirred for 5 days. The reaction mixture was poured into a mixture of 100 mL of ice and 150 mL of 1 M HCl and extracted with DCM. The organic phase was washed with saturated $NaHCO_3$ solution, water, and brine, dried over $MgSO_4$, and evaporated. The product was purified with column chromatography (mobile phase: isohexane 15% in DCM). The para product, **7b** (1.78 g, 42%), was isolated as a yellow oil. Anal. ($C_{16}H_{13}NO_6$) C, H, N.

3-(4-Methoxybenzyl)-5-nitromethylbenzoate (8b). Starting from compound **7b** (2.37 g, 7.53 mmol), compound **8b** was prepared as described above for **8a** except that the reaction mixture was stirred at room temperature overnight instead of being refluxed for 6 h. The product **8b** was isolated as an off-white solid (1.62 g, 71%). Anal. ($C_{16}H_{15}NO_5$) C, H, N.

3-(4-Methoxybenzyl)-5-nitrobenzoic Acid (13). A solution of **8b** (1.62 g, 5.37 mmol) was prepared in THF (95 mL), H_2O (27 mL), and MeOH (13.5 mL). A sample of 1 M LiOH (27 mL) was added slowly. The reaction mixture was left stirring at room temperature overnight, then concentrated, diluted with water, and acidified with 6 M HCl. The aqueous solution was extracted with ethyl acetate. The organic phase was washed with water and brine, dried with $MgSO_4$, and evaporated. Product **13** was isolated as a clear oil (1.38 g, 89%). Anal. ($C_{15}H_{13}NO_5$) C, H, N.

3-(9*H*-Fluoren-9-ylmethoxycarbonylamino)-5-(4-methoxybenzyl)benzoic Acid (14). A round-bottom flask was charged with a solution of **13** (250 mg, 0.87 mmol) in methanol (15 mL). Palladium on charcoal (10%, 90 mg, 0.087 mmol) was added to the flask, which was sealed with a septum and purged with nitrogen and then with hydrogen gas. The reaction mixture was stirred under hydrogen at atmospheric pressure for 60 min and was then filtered and evaporated. The raw product was analyzed by LC−MS and used without further purification. The generated aniline (0.87 mmol) was dissolved in dioxane (10 mL) and cooled in an ice bath. An aqueous solution of Na_2CO_3 (0.3 M, 10 mL) was added slowly. Fmoc chloride (248 mg, 0.96 mmol) was dissolved in dioxane (10 mL) and added dropwise to the reaction mixture, which was allowed to attain ambient temperature under stirring for 40 h. The reaction mixture was acidified slowly with 6 M HCl and partitioned between water and ethyl acetate. The water phase was extracted further with ethyl acetate. All organic phases were pooled, washed with water and brine, dried with $MgSO_4$, and evaporated. The product was purified by silica column chromatography using ethyl acetate/isohexane/formic acid (49:50:1) and was eluated from the column with methanol. The eluate was evaporated and then distributed between ethyl acetate and water. The organic phase was dried and evaporated to yield **14** (204 mg, 49%). Anal. ($C_{30}H_{25}NO_5 \cdot {}^1/_3H_2O$) C, N. H: calcd, 5.33; found 4.8.

3-(9*H*-Fluoren-9-ylmethoxycarbonylamino)-5-(4-hydroxybenzyl)benzoic Acid (15). Compound **15** was prepared from **14** (500 mg, 1.04 mmol) according to the procedure outlined for compound **12** except for the workup and purification, which were modified. The reaction mixture was poured into 1 M HCl (100 mL) and extracted into ethyl acetate. The organic phase was washed with $NaHCO_3$, water, and brine, dried with Na_2SO_4, and evaporated. The product was purified by RP-HPLC using a 40 min gradient of 40−85% CH_3CN in 0.05% aqueous formic acid and gave, after freeze-drying, **15** as a white solid (288 mg, 59%). Anal. ($C_{29}H_{23}NO_5 \cdot H_2O$) C, H, N.

General Synthesis of Angiotensin Analogues. Coupling. Fmoc-His(Trt)-Pro-Phe-Wang resin (1 equiv) was weighed into a 2 mL disposable syringe equipped with a porous polyethylene filter and allowed to swell in DMF (1.5 mL) for 1 h. The Fmoc group was removed by a three-step treatment with 20% piperidine in DMF (3 × 1.5 mL, 1 + 3 + 10 min), and the polymer was washed with DMF (6 × 1.5 mL, 6 × 1 min). The turn scaffold, **12** or **15** (1.25 equiv), and PyBOP (1.25 equiv) were dissolved in DMF (1.5 mL) in the presence of DIEA (2.5 equiv) and allowed to react with the resin overnight (18 h). LC−MS analysis after cleavage of an analytical sample showed complete reaction. The rest of the resin was washed with DMF (6 × 2 mL, 6 × 1 min). The Fmoc group was cleaved as described above, and the resin was washed with DMF (6 × 2 mL, 6 × 1 min), DCM (5 × 2 mL, 5 × 1 min), and MeOH (5 × 2 mL, 5 × 1 min) before it was dried in a vacuum overnight. An aliquot of the resin was swelled in DMF (2 mL). The appropriate acid (5 equiv) was dissolved with PyBOP (5 equiv) and DIEA (10 equiv) in DMF (0.5 mL). The solution was added to the resin and agitated by rotation overnight. In all cases, LC−MS analysis of a cleaved sample showed complete reaction. The resin was washed, and the Fmoc group was cleaved as described above. Coupling of additional amino acids was conducted as described above, but the reaction time was shortened to 2 h. The resin was deprotected, washed, and dried as above.

Cleavage. To cleave the peptide from the resin, triethylsilane (100 μL) and 95% aqueous TFA (1.5 mL) were added, and the mixture was agitated for 1 h. The polymer was filtered off and washed with TFA (2 × 0.3 mL). The filtrate was evaporated in a stream of nitrogen, and the product was precipitated by addition of diethyl ether (13 mL). The precipitate was collected by centrifugation, washed with ether (3 × 7 mL), and dried.

Purification. The crude peptide, unless otherwise stated, was dissolved in MeCN (0.4 mL) and H_2O (3.6 mL) and purified in two runs by RP-HPLC on a 10 μm Vydac C18 column (2.2 cm × 25 cm) with a 90 min gradient of 15−45% MeCN in 0.1% aqueous TFA at a flow rate of 5 mL/min. The separation was monitored at 230 nm by analytical RP-HPLC and/or LC−MS of selected fractions.

Analogues 1 and 2. The synthesis of these compounds has been described earlier.[27]

Analogue 3. An aliquot (53 mg, 28 μmol) of the resin obtained after introduction of template **12** was coupled with Fmoc-Val-OH (140 μmol) and deprotected according to the general procedure. The peptide chain was further elongated by successive couplings of Fmoc-Arg(Pbf)-OH and Fmoc-Asp(O*t*-Bu)-OH in the same manner but using reaction times of 2.5 h. After removal of the Fmoc group and after being washed and dried, the product was cleaved from the resin by treatment with triethylsilane and 95% aqueous TFA as described above. The crude product, dissolved in 2.2 mL of 10% MeCN, was purified by RP-HPLC on a 5 μm ACE phenyl column (21.2 mm

× 150 mm) using a 60 min gradient of 10−40% MeCN in 0.1% aqueous TFA and a flow rate of 5 mL/min. Yield: 6.6 mg (17%). LC−MS (M_{abs} = 1008.48): 1009.3 (M + H^+), 505.4 ([M + $2H^+$]/2), 337.3 ([M + $3H^+$]/3), 350.9 ([M + MeCN + $3H^+$]/3). Amino acid analysis: Asp, 0.99; Arg, 1.01; Val, 0.70; His, 0.98; Pro, 1.01; Phe, 0.98.

Analogue 4. After incorporation of scaffold **15**, an aliquot of the resin (75 mg, 40 μmol) was subjected to successive couplings with Fmoc-Arg(Pbf)-OH (200 μmol) and Fmoc-Asp(O*t*-Bu)-OH (200 μmol) as outlined above. The product was cleaved and purified according to the standard procedures to yield 14.9 mg (26%). LC−MS (M_{abs} = 895.4): 448.9 ([M + $2H^+$]/2). Amino acid analysis: Asp, 0.97; Arg, 0.99; His, 1.01; Pro, 1.03; Phe, 1.00.

Analogue 5. A second aliquot of the same resin (75 mg, 40 μmol) was coupled seqentially with Fmoc-Val-OH (200 μmol), Fmoc-Arg(Pbf)-OH (200 μmol), and Fmoc-Asp(O*t*-Bu)-OH (200 μmol) as described above. Standard cleavage and purification yielded 6.9 mg (11%). LC−MS (M_{abs} = 994.6): 498.6 ([M + $2H^+$]/2), 346.4 ([M + MeCN + $3H^+$]/3). Amino acid analysis: Asp, 0.99; Arg, 0.99; Val, 0.98; His, 1.01; Pro, 1.02; Phe, 1.01.

Rat Liver Membrane AT_1 Receptor Binding Assay. Rat liver membranes were prepared according to the method of Dudley et al.[42] Binding of [^{125}I]Ang II to membranes was conducted in a final volume of 0.5 mL containing 50 mM Tris-HCl (pH 7.4), 100 mM NaCl, 10 mM $MgCl_2$, 1 mM EDTA, 10 μM bacitracin, 10 μM pepstatin A, 10 μM bestatin, 10 μM captopril, 0.2% BSA (bovine serum albumin), liver homogenate corresponding to 5 mg of the original tissue weight, [^{125}I]Ang II (80 000 cpm, 0.03 nM), and variable concentrations (0.01 nM to 1.0 μM) of test substance. Samples were incubated at 25 °C for 2 h, and binding was terminated by filtration through Whatman GF/B glass-fiber filter sheets using a Brandel cell harvester. The filters were washed with 3 × 3 mL of Tris-HCl (pH 7.4) and transferred to tubes. The radioactivity was measured with a γ-counter. Nonspecific binding was determined in the presence of 1 μM Ang II. The specific binding was determined by subtracting the nonspecific binding from the total bound [^{125}I]Ang II. IC_{50} was determined by Scatchard analysis of data obtained with Ang II by using GraFit (Erithacus Software, U.K.). The apparent dissociation constants K_i were calculated from IC_{50} values using the Cheng−Prusoff equation[54] (K_d = 1.7 ± 0.1 nM, [L] = 0.057 nM). The binding data were best fitted with a one-site fit. All experiments were performed in triplicate.

Pig Myometrial Membrane AT_2 Receptor Binding Assay. Myometrial membranes were prepared from porcine uteri according to the method of Nielsen et al.[43] Potential interference by binding to AT_1 receptors was blocked by addition of 1 μM losartan. Binding of [^{125}I]Ang II to membranes was conducted in a final volume of 0.5 mL containing 50 mM Tris-HCl (pH 7.4), 100 mM NaCl, 10 mM $MgCl_2$, 1 mM EDTA, 10 μM bacitracin, 10 μM pepstatin A, 10 μM bestatin, 10 μM captopril, 0.2% BSA, homogenate corresponding to 10 mg of the original tissue weight, [^{125}I]Ang II (80 000 cpm, 0.03 mM), and variable concentrations (0.01 nM to 1.0 μM) of test substance. Samples were incubated at 25 °C for 1.5 h, and binding was terminated by filtration through Whatman GF/B glass-fiber filter sheets using a Brandel cell harvester. The filters were washed with 3 × 3 mL of Tris-HCl (pH 7.4) and transferred to tubes. The radioactivity was measured with a γ-counter. Nonspecific binding was determined in the presence of 1 μM Ang II. The specific binding was determined by subtracting the nonspecific binding from the total bound [^{125}I]-Ang II. IC_{50} was determined by Scatchard analysis of data obtained with Ang II by using GraFit (Erithacus Software, U.K.). The apparent dissociation constants K_i were calculated using the Cheng−Prusoff equation[54] (K_d = 0.7 ± 0.1 nM, [L] = 0.057 nM). The binding data were best fitted with a one-site fit. All experiments were performed in triplicate.

In Vitro Morphological Effects. NG108-15 cells (provided by Drs. M. Emerit and M. Hamon; INSERM, U. 238, Paris, France) were cultured (passage 18−28) in Dulbecco's modified Eagle's medium (DMEM, Gibco BRL, Burlington, Ontario, Canada) with 10% fetal bovine serum (FBS, Gibco), HAT supplement (hypoxanthine, aminopterin, thymidine from Gibco), and 50 mg/L gentamycin (Gibco) at 37 °C in 75 cm^2 Nunclon Delta flasks in a humidified atmosphere of 93% air and 7% CO_2, as previously described.[44] Subcultures were formed at subconfluency. Under these conditions, cells express only the AT_2 receptor subtype.[44,45] Cells were stimulated for 3 days, once a day (first stimulation 24 h after plating). Cells were cultured for 3 subsequent days under these conditions. For all experiments, cells were plated at the same initial density of 6 × 10^4 cells /35 mm Petri dish. Cells were treated without (control cells) and with [Val^5]angiotensin II from Bachem (Marina Delphen, CA) (100 nM) or **5** (100 nM) and in the absence or in the presence of PD 123,319 (RBI Natick, MA) (1 μM), an AT_2 receptor antagonist introduced daily 30 min prior to Ang II or **5**.

Determination of Cells with Neurites. Cells were examined daily under a phase contrast microscope, and micrographs were taken after 3 days under the various experimental conditions. Cells with at least one neurite longer than a cell body were counted as positive for neurite outgrowth. At least 140 cells were counted in three independent experiments.[9]

Vascular Contractility Studies. This study was performed at Cerep (France) according to literature.[46] Seven concentrations (3, 10, 30, 100, 300, 1000, 3000 nM) of **5** were tested. Ang II was used as a reference agonist, and saralasin (0.03 μM) was used as a reference antagonist.

Conformational Analysis and Molecular Modeling. General Protocol for Conformational Analysis. The conformational search was conducted using the systematic unbound multiple minimum (SUMM) search method[55] in the BatchMin program. The OPLS-AA force field and the general Born solvent accessible (GB/SA) surface area method for water developed by Still et al.,[56] as implemented in the program MacroModel 8.5,[57] were used in the calculations. The number of torsion angles allowed to vary simultaneously during each Monte Carlo step ranged from 1 to n − 1. Amide bonds were fixed in the trans configuration. Truncated Newton conjugate gradient (TNCG) minimization with a maximum of 500 iterations was used in the conformational search, with the derivative convergence set to 0.05 kJ mol^{-1} $Å^{-1}$. Torsional memory was used. All heavy atoms were used in the comparison for unique conformations, if nothing else is stated. Conformations within 5 kcal/mol of the lowest energy minimum were kept. The obtained conformations were subsequently minimized with derivative convergence set to 0.001 kJ mol^{-1} $Å^{-1}$ using TNCG minimization with a maximum of 500 iterations.

Comparison of Scaffolds to γ-Turns in Protein Crystal Structures. Conformational analysis of compounds of **F** and **G** modified with an N-terminal acetyl cap, C-terminal *N*-methylamide cap, and an alanine side chain instead of the tyrosine side chain was performed according to the general protocol above with 1000 search steps per rotatable bond. The conformations identified within 5 kcal/mol of the lowest found minimum of the model compound of **F** (eight conformations) and **G** (four conformations) were compared to 2101 inverse γ-turns (defined as ideal angles ±30°), extracted from a representative set of crystallized proteins selected using the PDB_SELECT list[58,59] from December 2003. The comparison was performed by least-squares alignment of $C_{\alpha i-1}$, $C_{\alpha i+1}$, $C_{\beta i+1}$, and $C_{\alpha i+3}$ in the protein turns and the corresponding atoms in the model compounds.

DISCOtech Analysis. The conformational search of structures **1m**, **3m**, **5m**, **16m**, **17m**, and **18m** was performed according to the general protocol above. The number of steps was set to 2000 per rotatable bond. The low-energy inverse γ-turn-like conformation was used for the ring system of the benzodiazepine-based scaffolds and was not searched. To reduce the number of identified conformations, all conformations with a distance of 4 Å or less between the carbon in the guanidino group and any oxygen atom were removed because there is support for the interaction of the Arg^2 side chain with Asp^{297} in the AT_2 receptor.[60] The criterion for unique confor-

mations was also changed from the default maximum distance of 0.25 Å to 1.0 Å between the compared atoms after superposition (CRMS). The compared atoms were (1) the methyl carbon of the N-terminal cap, (2) the arginine C_α, (3) the carbon in the guanidino group, (4) the tyrosine C_α (the aromatic carbon in **1m**, **3m** and **5m**), (5) the tyrosine phenolic oxygen atom, and (6) the methyl carbon of the C-terminal cap. The number of conformations found within 5 kcal/mol of the energy minimum for **1m**, **3m**, **5m**, **16m**, **17m**, and **18m** were 590, 1159, 2865, 1963, 893, and 772, respectively. Owing to the limit in the number of conformations that DISCOtech[48] can handle (≤300 conformations per molecule), only conformations of a compound that could superimpose selected atoms with a low rms atomic distance to the conformations of the other compounds were used. The superimposed atoms were the same as the atoms used for comparison in the conformational analysis. In our previous DISCOtech analysis,[24] the conformations selected and used were based on conformational diversity. In the present study, intermolecular conformational similarity was used to select conformations for the DISCOtech analysis. We believe that this approach of selecting conformations makes it easier to obtain good alignments in DISCOtech. One-hundred-thirty-four conformations of **3m** that all could be superimposed with an rms atomic pair distance below 1.5 Å onto any conformation of **17m** and **18m** were used as reference conformations. These conformations were aligned to all the conformations of the other compounds to guide the selection of conformations to include in DISCOtech. For **18m**, 360 conformations were superimposed with an rms distance below 1.5 Å onto the reference set. Of these, the 300 conformations with the lowest energy were selected. For **5m**, 807 conformations matched but were reduced to 265 by decreasing the rms distance criterion to 1.1 Å. Owing to a very low number of matched conformations of **16m**, the rms distance criterion was set to 2.2 Å for this compound, giving 100 conformations. The number of conformations that matched the reference set for **1m** (159) and **17m** (268) was within the DISCOtech limit using the 1.5 Å criterion.

The DISCOtech module in SYBYL,version 6.9,[61] was used to find an alignment of selected structural elements. The selected structural elements were (1) the methyl carbon of the N-terminal cap (corresponding to C_α in the aspartic acid in the full-length pseudopeptide), (2) the receptor acceptor sites originating from the guanidino group (as defined by DISCOtech), (3) the tyrosine phenolic oxygen atom, and (4) the methyl carbon of the C-terminal cap (corresponding to C_α in the histidine in the full-length pseudopeptide). Different DISCOtech features were created for the tyrosine phenolic oxygen atom and the capped ends by transforming relevant atoms into DISCOtech recognizable features. The hydrogen atoms of the acetyl capping group were transformed into carbons, thus creating a hydrophobic *tert*-butyl feature. The methyl group of the C-terminal cap was transformed into a quaternary nitrogen group, thus creating a positively charged feature. The nitrogen atoms in the guanidino group were transformed into oxygen atoms, thus creating a unique feature from where only DISCOtech acceptor site features can be obtained. The tyrosine phenolic oxygen atom was transformed into a quaternary nitrogen atom and defined as a unique feature, thus removing the potential DISCOtech acceptor site feature. To simplify the procedure, all atoms not included in a feature were transformed into hydrogen atoms. In the transformations only the atom types were changed, not the geometry. The DISCOtech setting "features by class" was used to search for models containing (1) more than zero acceptor sites (receptor points corresponding to the guanidino group), (2) one hydrophobic feature (the transformed feature corresponding to the C_α of the aspartic acid residue in the full-length pseudopeptides), (3) one tyrosine phenolic oxygen atom, and (4) one positively charged nitrogen atom (the transformed feature corresponding to C_α of the histidine residue). The tolerance for a feature match between the molecules was set from 0.25 to 2.5 Å in increments of 0.25 Å if no models were found at the lower tolerance. DISCOtech was set to obtain models where all or all but one compound were included. **17m**, corresponding to the pseudopeptide with the highest affinity, was used as the reference molecule.

The DISCOtech analysis with only the AT_2 receptor agonist model compounds **5m**, **16m**, **17m**, and **18m** included was made using the same DISCOtech protocol. The reference set for selecting similar conformations among the different compounds consisted of the conformations of **17m** that could be superimposed with an rms atomic pair distance below 1.5 Å onto any conformation of **5m** and **18m** and below 2.2 Å onto any conformations of **16m**. Included conformations of **5m** were those that could be superimposed onto the reference set with an rms atomic pair distance below 1.25 Å. For **16m** and **18m** the rms distance criterion was set to 2.2 and 1.5 Å, respectively.

Acknowledgment. We gratefully acknowledge the financial support from the Swedish Research Council and the Swedish Foundation for Strategic Research. We also thank Biotage AB for providing the Smith microwave synthesizer.

Supporting Information Available: ^{1}H and ^{13}C NMR spectral data of compounds **7a**,**b**, **8a**,**b**, and **9**−**15**, MS, LC−MS, and IR data, elemental analysis results of all new compounds, purity determination and HRMS data for the pseudopeptides **1**−**5**, and ^{1}H NMR data for **3** and **4**. This material is available free of charge via the Internet at http://pubs.acs.org.

References

(1) De Gasparo, M.; Catt, K. J.; Inagami, T.; Wright, J. W.; Unger, T. International Union of Pharmacology. XXIII. The Angiotensin II Receptors. *Pharmacol. Rev.* **2000**, *52*, 415−472.
(2) Kaschina, E.; Unger, T. Angiotensin AT1/AT2 Receptors: Regulation, Signalling and Function. *Blood Pressure* **2003**, *12*, 70−88.
(3) Timmermans, P. B. M. W. M.; Wong, P. C.; Chiu, A. T.; Herblin, W. F.; Benfield, P.; Carini, D. J.; Lee, R. J.; Wexler, R. R.; Saye, J. A. M.; Smith, R. D. Angiotensin II Receptors and Angiotensin II Receptor Antagonists. *Pharmacol. Rev.* **1993**, *45*, 205−251.
(4) Mukoyama, M.; Nakajima, M.; Horiuchi, M.; Sasamura, H.; Pratt, R. E.; Dzau, V. J. Expression Cloning of Type 2 Angiotensin II Receptor Reveals a Unique Class of Seven-Transmembrane Receptors. *J. Biol. Chem.* **1993**, *268*, 24539−24542.
(5) Kambayashi, Y.; Bardhan, S.; Takahashi, K.; Tsuzuki, S.; Inui, H.; Hamakubo, T.; Inagami, T. Molecular Cloning of a Novel Angiotensin II Receptor Isoform Involved in Phosphotyrosine Phosphatase Inhibition. *J. Biol. Chem.* **1993**, *268*, 24543−24546.
(6) Widdop, R. E.; Jones, E. S.; Hannan, R. E.; Gaspari, T. A. Angiotensin AT2 Receptors: Cardiovascular Hope or Hype? *Br. J. Pharmacol.* **2003**, *140*, 809−824.
(7) Johansson, B.; Holm, M.; Ewert, S.; Casselbrant, A.; Pettersson, A.; Fändriks, L. Angiotensin II Type 2 Receptor-Mediated Duodenal Mucosal Alkaline Secretion in the Rat. *Am. J. Physiol.* **2001**, *280*, G1254−G1260.
(8) Gendron, L.; Payet, M. D.; Gallo-Payet, N. The Angiotensin Type 2 Receptor of Angiotensin II and Neuronal Differentiation: From Observations to Mechanisms. *J. Mol. Endocrinol.* **2003**, *31*, 359−372.
(9) Gendron, L.; Coté, F.; Payet, M. D.; Gallo-Payet, N. Nitric Oxide and Cyclic GMP Are Involved in Angiotensin II AT(2) Receptor Effects on Neurite Outgrowth in NG108-15 Cells. *Neuroendocrinology* **2002**, *75*, 70−81.
(10) Gendron, L.; Laflamme, L.; Rivard, N.; Asselin, C.; Payet, M. D.; Gallo-Payet, N. Signals from the AT2 (Angiotensin Type 2) Receptor of Angiotensin II Inhibit p21ras and Activate MAPK (Mitogen-Activated Protein Kinase) To Induce Morphological Neuronal Differentiation in NG108-15 Cells. *Mol. Endocrinol.* **1999**, *13*, 1615−1626.
(11) Jöhren, O.; Dendorfer, A.; Dominiak, P. Cardiovascular and Renal Function of Angiotensin II Type-2 Receptors. *Cardiovasc. Res.* **2004**, *62*, 460−467.
(12) Steckelings, U. M.; Kaschina, E.; Unger, T. The AT2 Receptor-A Matter of Love and Hate. *Peptides* **2005**, *26*, 1401−1409.
(13) Nikiforovich, G. V.; Marshall, G. R. Three-Dimensional Recognition Requirements for Angiotensin Agonists: A Novel Solution for an Old Problem. *Biochem. Biophys. Res. Commun.* **1993**, *195*, 222−228.

(14) Samanen, J. M.; Peishoff, C. E.; Keenan, R. M.; Weinstock, J. Refinement of a Molecular-Model of Angiotensin-II (AII) Employed in the Discovery of Potent Nonpeptide Antagonists. *Bioorg. Med. Chem. Lett.* **1993**, *3*, 909−914.
(15) Nikiforovich, G. V.; Kao, J. L. F.; Plucinska, K.; Zhang, W. J.; Marshall, G. R. Conformational Analysis of Two Cyclic Analogs of Angiotensin: Implications for the Biologically Active Conformation. *Biochemistry* **1994**, *33*, 3591−3598.
(16) Boucard, A. A.; Wilkes, B. C.; Laporte, S. A.; Escher, E.; Guillemette, G.; Leduc, R. Photolabeling Identifies Position 172 of the Human AT1 Receptor as a Ligand Contact Point: Receptor-Bound Angiotensin II Adopts an Extended Structure. *Biochemistry* **2000**, *39*, 9662−9670.
(17) Matsoukas, J. M.; Polevaya, L.; Ancans, J.; Mavromoustakos, T.; Kolocouris, A.; Roumelioti, P.; Vlahakos, D. V.; Yamdagni, R.; Wu, Q.; Moore, G. J. The Design and Synthesis of a Potent Angiotensin II Cyclic Analogue Confirms the Ring Cluster Receptor Conformation of the Hormone Angiotensin II. *Bioorg. Med. Chem.* **2000**, *8*, 1−10.
(18) Plucinska, K.; Kataoka, T.; Yodo, M.; Cody, W. L.; He, J. X.; Humblet, C.; Lu, G. H.; Lunney, E.; Major, T. C.; et al. Multiple Binding Modes for the Receptor-Bound Conformations of Cyclic AII Agonists. *J. Med. Chem.* **1993**, *36*, 1902−1913.
(19) Printz, M. P.; Nemethy, G.; Bleich, H. Proposed Models for Angiotensin II in Aqueous Solution and Conclusions about Receptor Topography. *Nature (London)* **1972**, *237*, 135−140.
(20) Spear, K. L.; Brown, M. S.; Reinhard, E. J.; McMahon, E. G.; Olins, G. M.; Palomo, M. A.; Patton, D. R. Conformational Restriction of Angiotensin II: Cyclic Analogs Having High Potency. *J. Med. Chem.* **1990**, *33*, 1935−1940.
(21) Schmidt, B.; Lindman, S.; Tong, W.; Lindeberg, G.; Gogoll, A.; Lai, Z.; Thoernwall, M.; Synnergren, B.; Nilsson, A.; Welch, C. J.; Sohtell, M.; Westerlund, C.; Nyberg, F.; Karlén, A.; Hallberg, A. Design, Synthesis, and Biological Activities of Four Angiotensin II Receptor Ligands with γ-Turn Mimetics Replacing Amino Acid Residues 3−5. *J. Med. Chem.* **1997**, *40*, 903−919.
(22) Deraet, M.; Rihakova, L.; Boucard, A.; Perodin, J.; Sauve, S.; Mathieu, A. P.; Guillemette, G.; Leduc, R.; Lavigne, P.; Escher, E. Angiotensin II Is Bound to Both Receptors AT1 and AT2, Parallel to the Transmembrane Domains and in an Extended Form. *Can. J. Physiol. Pharmacol.* **2002**, *80*, 418−425.
(23) Rosenström, U.; Sköld, C.; Lindeberg, G.; Botros, M.; Nyberg, F.; Karlén, A.; Hallberg, A. A Selective AT2 Receptor Ligand with a γ-Turn-like Mimetic Replacing the Amino Acid Residues 4−5 of Angiotensin II. *J. Med. Chem.* **2004**, *47*, 859−870.
(24) Rosenström, U.; Sköld, C.; Plouffe, B.; Lindeberg, G.; Botros, M.; Nyberg, F.; Wolf, G.; Karlén, A.; Gallo-Payet, N.; Hallberg, A. New Selective AT2 Receptor Ligands Encompassing a γ-Turn Mimetic Replacing the Amino Acid Residues 4−5 of Angiotensin II Act as Agonists. *J. Med. Chem.* **2005**, *48*, 4009−4024.
(25) Lindman, S.; Lindeberg, G.; Frändberg, P.-A.; Nyberg, F.; Karlén, A.; Hallberg, A. Effect of 3−5 Monocyclizations of Angiotensin II and 4-AminoPhe6-Ang II on AT2 Receptor Affinity. *Bioorg. Med. Chem.* **2003**, *11*, 2947−2954.
(26) Lindman, S.; Lindeberg, G.; Gogoll, A.; Nyberg, F.; Karlén, A.; Hallberg, A. Synthesis, Receptor Binding Affinities and Conformational Properties of Cyclic Methylenedithioether Analogues of Angiotensin II. *Bioorg. Med. Chem.* **2001**, *9*, 763−772.
(27) Lindman, S.; Lindeberg, G.; Nyberg, F.; Karlén, A.; Hallberg, A. Comparison of Three γ-Turn Mimetic Scaffolds Incorporated into Angiotensin II. *Bioorg. Med. Chem.* **2000**, *8*, 2375−2383.
(28) Olah, G. A.; Overchuk, N. A. Aromatic Substitution. XXV. Selectivity in the Friedel−Crafts Benzylation, Isopropylation, and *tert*-Butylation of Benzene and Toluene. *J. Am. Chem. Soc.* **1965**, *87*, 5786−5788.
(29) Babiak, K. A.; Carpenter, A.; Chou, S.; Colson, P.-J.; Farid, P.; Hett, R.; Huber, C. H.; Koeller, K. J.; Lawson, J. P.; Li, J.; Mar, E. K.; Miller, L. M.; Orlovski, V.; Peterson, J. C.; Pozzo, M. J.; Przybyla, C. A.; Tremont, S. J.; Trivedi, J. S.; Wagner, G. M.; Weisenburger, G. A.; Zhi, B. PCT Int. Appl. 2001068637, 2001.
(30) Waterlot, C.; Couturier, D.; De Backer, M.; Rigo, B. A Study of Hydrogenation of Benzhydrols in the Presence of Catalytic Amount of Triflic Acid. *Can. J. Chem.* **2000**, *78*, 1242−1246.
(31) Olah, G. A.; Arvanaghi, M.; Ohannesian, L. Synthetic Methods and Reactions. 126. Trifluoromethanesulfonic Acid/Triethylsilane: A New Ionic Hydrogenation Reagent for the Reduction of Diaryl and Alkyl Aryl Ketones to Hydrocarbons. *Synthesis,* **1986**, 770−772.
(32) Georgsson, J.; Hallberg, A.; Larhed, M. Rapid Palladium-Catalyzed Synthesis of Esters from Aryl Halides Utilizing Mo$(CO)_6$ as a Solid Carbon Monoxide Source. *J. Comb. Chem* **2003**, *5*, 350−352.
(33) Alterman, M.; Hallberg, A. Fast Microwave-Assisted Preparation of Aryl and Vinyl Nitriles and the Corresponding Tetrazoles from Organo-halides. *J. Org. Chem.* **2000**, *65*, 7984−7989.
(34) Tschaen, D. M.; Desmond, R.; King, A. O.; Fortin, M. C.; Pipik, B.; King, S.; Verhoeven, T. R. An Improved Procedure for Aromatic Cyanation. *Synth. Commun.* **1994**, *24*, 887−890.
(35) Sundermeier, M.; Zapf, A.; Beller, M. A Convenient Procedure for the Palladium-Catalyzed Cyanation of Aryl Halides. *Angew. Chem., Int. Ed.* **2003**, *42*, 1661−1664.
(36) Neustadt, B. R.; Smith, E. M.; Nechuta, T.; Zhang, Y. Combinatorial Libraries Based on a Novel and Readily Accessible "Centroid" Scaffold. *Tetrahedron Lett.* **1998**, *39*, 5317−5320.
(37) McOmie, J. F. W.; Watts, M. L.; West, D. E. Demethylation of Aryl Methyl Ethers by Boron Tribromide. *Tetrahedron,* **1968**, *24*, 2289−2292.
(38) Mueller, L. PE-COSY, a Simple Alternative to E-COSY. *J. Magn. Reson.* **1987**, *72*, 191−196.
(39) Braunschweiler, L.; Ernst, R. R. Coherence transfer by isotropic mixing: application to proton correlation spectroscopy. *J. Magn. Reson.* **1983**, *53*, 521−528.
(40) Bax, A.; Davis, D. G. Practical aspects of two-dimensional transverse NOE spectroscopy. *J. Magn. Reson.* **1985**, *63*, 207−213.
(41) Smallcombe, S. H.; Patt, S. L.; Keifer, P. A. WET solvent suppression and its applications to LC NMR and high-resolution NMR spectroscopy. *J. Magn. Reson.* **1995**, *117*, 295−303.
(42) Dudley, D. T.; Panek, R. L.; Major, T. C.; Lu, G. H.; Bruns, R. F.; Klinkefus, B. A.; Hodges, J. C.; Weishaar, R. E. Subclasses of Angiotensin II Binding Sites and Their Functional Significance. *Mol. Pharmacol.* **1990**, *38*, 370−377.
(43) Nielsen, A. H.; Schauser, K.; Winther, H.; Dantzer, V.; Poulsen, K. Angiotensin II Receptors and Renin in the Porcine Uterus: Myometrial AT2 and Endometrial AT1 Receptors Are Down-Regulated during Gestation. *Clin. Exp. Pharmacol. Physiol.* **1997**, *24*, 309−314.
(44) Buisson, B.; Bottari, S. P.; de Gasparo, M.; Gallo-Payet, N.; Payet, M. D. The Angiotensin AT2 Receptor Modulates T-Type Calcium Current in Non-Differentiated NG108-15 Cells. *FEBS Lett.* **1992**, *309*, 161−164.
(45) Laflamme, L.; Gasparo, M.; Gallo, J. M.; Payet, M. D.; Gallo-Payet, N. Angiotensin II Induction of Neurite Outgrowth by AT2 Receptors in NG108-15 Cells. Effect Counteracted by the AT1 Receptors. *J. Biol. Chem.* **1996**, *271*, 22729−22735.
(46) Pendleton, R. G.; Gessner, G.; Horner, E. Studies on Inhibition of Angiotensin II Receptors in Rabbit Adrenal and Aorta. *J. Pharmacol. Exp. Ther.* **1989**, *248*, 637−643.
(47) Berman, H. M.; Westbrook, J.; Feng, Z.; Gilliland, G.; Bhat, T. N.; Weissig, H.; Shindyalov, I. N.; Bourne, P. E. The Protein Data Bank. *Nucleic Acids Res.* **2000**, *28*, 235−242 (http://www.pdb.org/).
(48) Martin, Y. C.; Bures, M. G.; Danaher, E. A.; DeLazzer, J.; Lico, I.; Pavlik, P. A. A Fast New Approach to Pharmacophore Mapping and Its Application to Dopaminergic and Benzodiazepine Agonists. *J. Comput.-Aided Mol. Des.* **1993**, *7*, 83−102.
(49) Huckle, W. R.; Kivlighn, S. D.; Zingaro, G. J.; Kevin, N.; Rivero, R. A.; Chang, R. S.; Greenlee, W. J.; Siegl, P. K. S.; Johnson, R. G. Angiotensin II Receptor-Mediated Activation of Phosphoinositide Hydrolysis and Elevation of Mean Arterial Pressure by Nonpeptide, L-163,491. *Can. J. Physiol. Pharmacol.* **1994**, *72* (Suppl. 1), 543.
(50) Wan, Y.; Wallinder, C.; Plouffe, B.; Beaudry, H.; Mahalingam, A. K.; Wu, X.; Johansson, B.; Holm, M.; Botoros, M.; Karlén, A.; Pettersson, A.; Nyberg, F.; Fändriks, L.; Gallo-Payet, N.; Hallberg, A.; Alterman, M. Design, Synthesis, and Biological Evaluation of the First Selective Nonpeptide AT2 Receptor Agonist. *J. Med. Chem.* **2004**, *47*, 5995−6008.
(51) Kivlighn, S. D.; Huckle, W. R.; Zingaro, G. J.; Rivero, R. A.; Lotti, V. J.; Chang, R. S. L.; Schorn, T. W.; Kevin, N.; Johnson, R. G., Jr. Discovery of L-162,313: a Nonpeptide that Mimics the Biological Actions of Angiotensin II. *Am. J. Physiol.* **1995**, *268*, R820−R823.
(52) Miura, S.-I.; Karnik, S. S. Angiotensin II Type 1 and Type 2 Receptors Bind Angiotensin II through Different Types of Epitope Recognition. *J. Hypertens.* **1999**, *17*, 397−404.
(53) Rosenström, U.; Sköld, C.; Lindeberg, G.; Botros, M.; Nyberg, F.; Hallberg, A.; Karlén, A. Synthesis and AT2 Receptor-binding Properties of Angiotensin II Analogues. *J. Pept. Res.* **2004**, *64*, 194−201.

(54) Cheng, Y.-C.; Prusoff, W. H. Relation between the Inhibition Constant (K_I) and the Concentration of Inhibitor Which Causes Fifty per Cent Inhibition (I_{50}) of an Enzymic Reaction. *Biochem. Pharmacol.* **1973**, *22*, 3099−3108.
(55) Goodman, J. M.; Still, W. C. An Unbounded Systematic Search of Conformational Space. *J. Comput. Chem.* **1991**, *12*, 1110−1117.
(56) Still, W. C.; Tempczyk, A.; Hawley, R. C.; Hendrickson, T. Semianalytical Treatment of Solvation for Molecular Mechanics and Dynamics. *J. Am. Chem. Soc.* **1990**, *112*, 6127−6129.
(57) Mohamadi, F.; Richards, N. G. J.; Guida, W. C.; Liskamp, R.; Lipton, M.; Caufield, C.; Chang, G.; Hendrickson, T.; Still, W. C. MacroModel, an Integrated Software System for Modeling Organic and Bioorganic Molecules Using Molecular Mechanics. *J. Comput. Chem.* **1990**, *11*, 440−467.
(58) Hobohm, U.; Sander, C. Enlarged Representative Set of Protein Structures. *Protein Sci.* **1994**, *3*, 522−524.
(59) Hobohm, U.; Scharf, M.; Schneider, R.; Sander, C. Selection of Representative Protein Data Sets. *Protein Sci.* **1992**, *1*, 409−417.
(60) Knowle, D.; Kurfis, J.; Gavini, N.; Pulakat, L. Role of Asp297 of the AT2 Receptor in High-Affinity Binding to Different Peptide Ligands. *Peptides* **2001**, *22*, 2145−2149.
(61) *SYBYL Molecular Modeling Software*, version 6.9; Tripos Inc. (1699 South Hanley Road, St. Louis, MO 63144).

JM050280Z